

ONSET OF THE 1979 SUMMER MONSOON - ECMWF LEVEL  
III-b ANALYSIS AND FORECAST EXPERIMENTS

P. Källberg

1. ANALYSIS

The monsoon onset over the Indian sub-continent during FGGE took place between June 11 and June 15, somewhat later than normal. Daily synoptic analyses of the FGGE II-b data indicate a major change of the circulation over large parts of the Indian Ocean and surrounding continents during these days. Synoptic analyses showing the surface pressure and 850 mb wind fields at June 11 12 GMT, (Figs. 1 and 2) and four days later, June 15 12 GMT, (Figs. 3 and 4) are presented.

A marked increase in the intensity of the westerlies over the Arabian Sea and a complete reversal of the flow over and south of the Mozambique channel are the major features to be noted. During these days the average kinetic energy over the Arabian Sea increased from  $5 \text{ m}^2 \text{ s}^{-2}$  to  $120 \text{ m}^2 \text{ s}^{-2}$  (Krishnamurty et al 1981). Cross sections along  $71^\circ \text{E}$ , Figs. 5 and 6 show both an increase, from  $6 \text{ ms}^{-1}$  to  $17 \text{ ms}^{-1}$ , and a northward displacement, from  $4^\circ \text{N}$  to  $9^\circ \text{N}$ , of the westerly wind maximum. The reversal of the circulation south of Madagascar was connected with a very rapid build-up of an anticyclone east of South Africa behind a rapidly filling polar front cyclone. The pressure at  $35^\circ \text{S}/35^\circ \text{E}$  rose more than 30 mb during the period, indeed the pressure was about 1030 mb at this position already on 12 GMT June 13.

The southerly outflow from this anticyclone towards the equator implies a dramatic extension southwards of the Somali jet, which on the 11th was well established only north of about  $5^\circ \text{S}$ . The monsoon onset is thus a large scale phenomenon affecting not only the Arabian Sea, but also the southern hemisphere part of the Indian ocean. The global scale of the reversal is well demonstrated in Fig. 7 which shows two week averages of the 200 mb velocity potentials immediately before (June 1-15) and after (June 16-30) the circulation change. There is a very marked intensification of the large

scale circulation cell with rising motion and upper level divergence over south-east Asia and upper level convergence and subsidence over the Mozambique region.

An interesting detail is the vortex that develops over the Arabian Sea, and has its centre at  $71^{\circ}\text{E}$   $14^{\circ}\text{N}$  on June 15. Such vortices are often, but not always, observed in connection with the very onset of the monsoon (Krishnamurti et al 1981). The vortex is well analysed from the FGGE data, as seen in the cross sections in Fig. 6 where a deeply penetrating cyclonic circulation with a cold lower core and a warm upper core has been analysed on June 15. The vortex persisted for several days, moving slowly towards northwest. The moist ascending air on the south side of the vortex was reported to give large amounts of precipitation.

## **2. FORECAST EXPERIMENTS**

A forecast experiment, using the operational version of the Centre's gridpoint model was run in an attempt to simulate the monsoon onset events. As initial data, the initialized analysis of June 11 12GMT was selected. Surface pressure and 850 mb wind forecasts at day D+4, June 15 12GMT are shown in Figs. 8 and 9. The verification is found in Figs. 3 and 4.

The forecast is remarkably successful in predicting the reversal of the circulation over the southern Indian ocean. Both the rapid build-up of an anticyclone, predicted maximum 1038 mb at  $35^{\circ}\text{E}/37^{\circ}\text{S}$ , and the southward extension of the Somali jet towards Mozambique and Madagascar are very well predicted. Even the small trough observed over the Comores on June 15 can be found in the forecast. The forecast over the Arabian Sea and Indian sub-continent is much less satisfactory. The monsoon onset vortex is completely absent, and the low level westerlies are much too weak. There is however a tendency of a northward displacement of the westerlies, similar but

less marked than that observed.

One problem encountered in the ECMWF data assimilation system is the inability of the non-linear normal mode initialization to retain large-scale divergence patterns in equatorial regions. With the availability of dense observations, such as cloud drift winds, the optimum interpolation is able to produce realistic large-scale divergences also in tropical regions (Julian 1981), but these divergences are heavily suppressed by the present 5-mode initialization.

A forecast experiment from the corresponding uninitialized analysis was made in order to assess the importance of initial state divergence for the medium range forecasts. Figures 10 and 11 show the 200 mb velocity potential before and after the initialization on June 11 12GMT. It is seen that the high latitude divergence patterns are relatively similar, but over equatorial regions the initialization effectively suppresses the divergence. The most marked difference is over Sumatra, where the divergence is reduced to about a third of its uninitialized value.

At high latitudes the two forecasts are virtually indistinguishable, Fig. 12. The curves show the relative anomaly correlation between the two forecasts poleward of 20°N. Even at day D+10 there is more than 95% correlation between the two forecasts in all wavenumber regimes. The same applies to the southern hemisphere.

Also in the tropics, Figs. 13 and 14, the two forecasts are very similar. The uninitialized forecast fails in predicting the eastward penetration of the Somali jet, and the onset vortex is again absent. There is however a stronger intensification of the southwesterlies over the bay of Bengal. Over the Comores-Mozambique area the two forecasts are very similar. From this comparison it is evident that the suppression of large-scale equatorial

divergence in the initial state is not the prime reason for the failure to forecast the monsoon onset over India.

It is well known that the Kuo cumulus parameterization scheme used in the present ECMWF model is very sensitive to the choice of the moisture storage parameter "b". This problem is discussed in Section 5.4. of the summary of this Workshop, where reference is made to an experiment carried out by M. Kanamitsu at ECMWF. In his experiment the coefficient "b" was altered by setting  $b=0$  and thereby letting all available moisture rain out immediately and thus supply its latent heat to the thermodynamics of the model. Figures 15 and 16 show the D+4 forecast from this experiment.

Now the monsoon is well developed over all of the Arabian Sea, and it has penetrated well beyond Sri Lanka, i.e. too far compared with the verification. A closed low, similar in structure to the onset vortex, but too far east, has developed over the Indian east coast. The circulation reversal over Mozambique is well predicted also in this case, and the trough over the Comores is more intense than in the other two forecasts. The extreme value of "b" makes it very easy for so called gridpoint storms to develop. One such small-scale disturbance can be seen at  $92^{\circ}\text{E}/20^{\circ}\text{S}$ .

#### **SUMMARY**

The dramatic change in large-scale circulation over the Indian Ocean area connected with the onset of the 1979 summer monsoon was well observed by the FGGE observational network. The ECMWF level III-b analyses show all the main features of the event. It may be noted that some special high density dropsonde and low level balloon data collected within the framework of Summer-MONEX were not available to us at the time of assimilation.

Some trial forecasts attempting to simulate the monsoon onset were only

moderately successful. A major reversal of the circulation over the Mozambique-Madagascar area is very well predicted, while the eastward penetration of the Somali jet towards India and the so called monsoon onset vortex, are not predicted satisfactorily. It is shown that the suppression of initial large-scale divergence by the non-linear normal mode initialization is not the primary reason for the failure. On the other hand, a very high sensitivity of the forecasts to the convection parameterization scheme is demonstrated.

#### **ACKNOWLEDGEMENT**

The experiments described here were made jointly by the ECMWF FGGE group.

#### **REFERENCES**

- Julian, P. 1981 An evaluation of the FGGE tropical observing system. GARP International conference on preliminary FGGE data analysis and results. Bergen, Norway 23-27 June 1980. WMO Geneva, April 1981, pp. 239-246.
- Krishnamurti, T.N., P. Ardanny, Y. Ramanathan, R.Pasch 1981 On the onset vortex of the summer monsoon. Mon.Wea.Rev., 109 pp. 344-363.

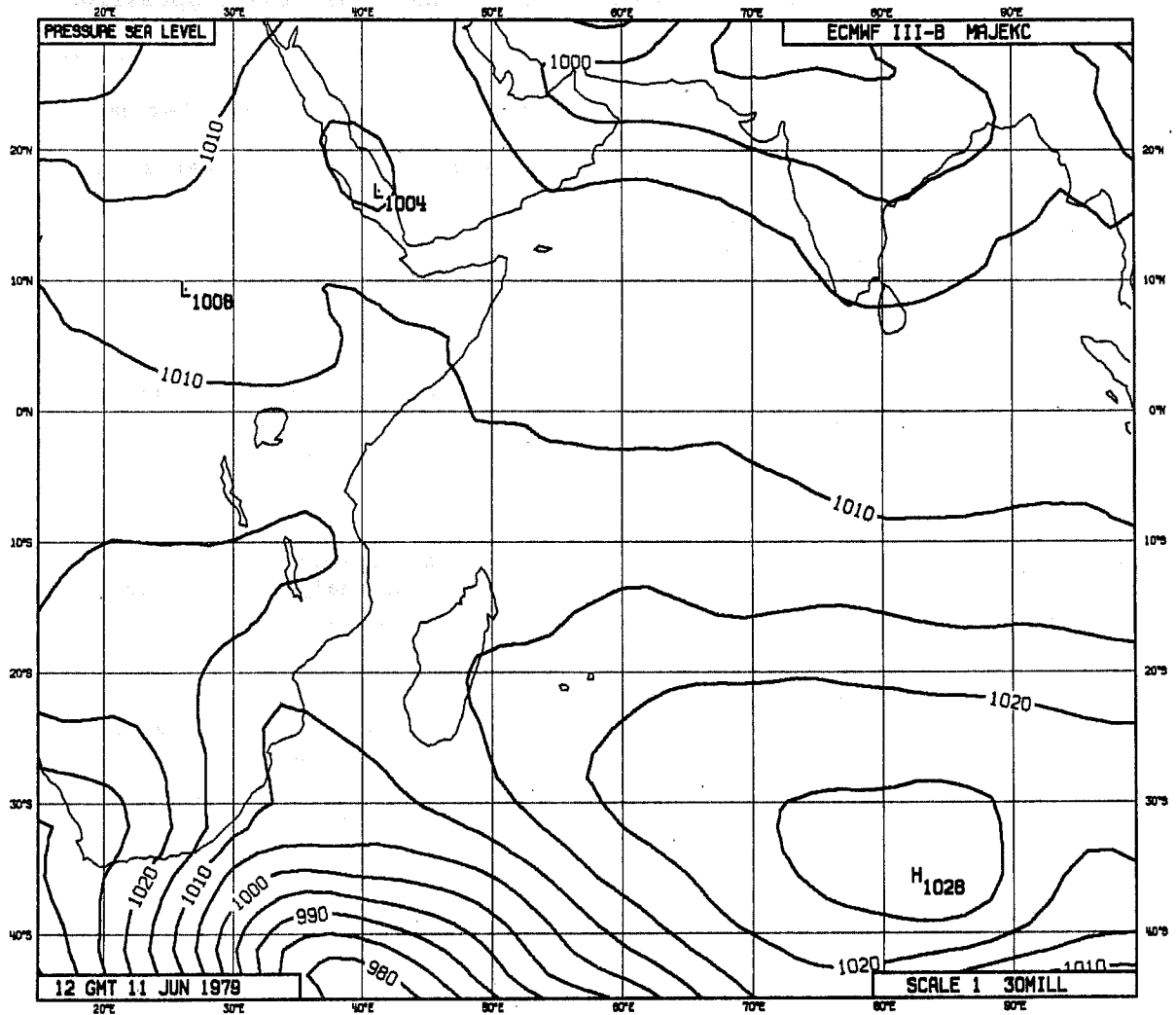


Fig. 1 Mean sea level pressure analysis, 12 GMT 11 June 1979. Contour interval 5 mb.

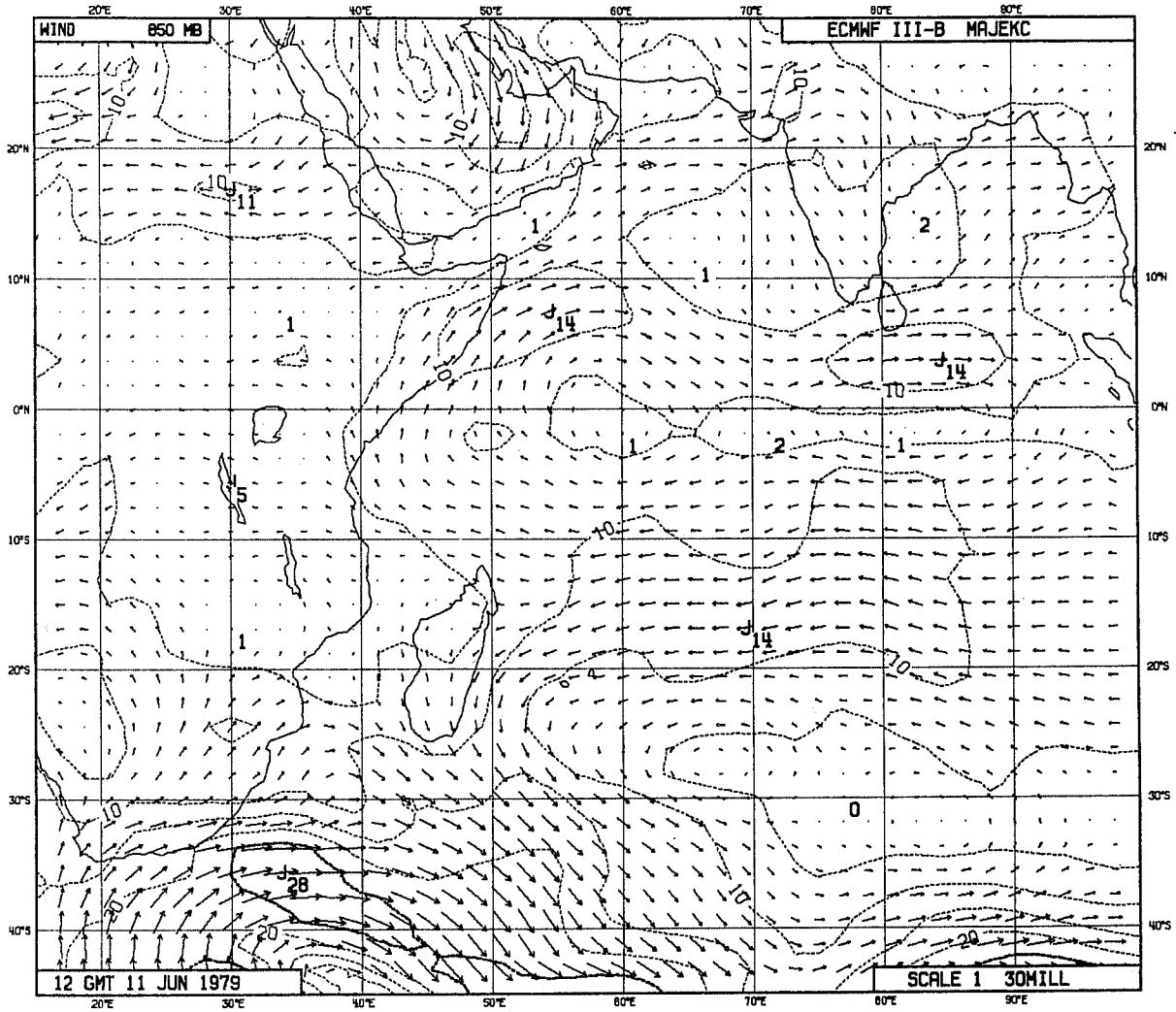


Fig. 2 850 mb wind analysis, 12 GMT 11 June 1979. Isotachs for every 5 ms<sup>-1</sup>.

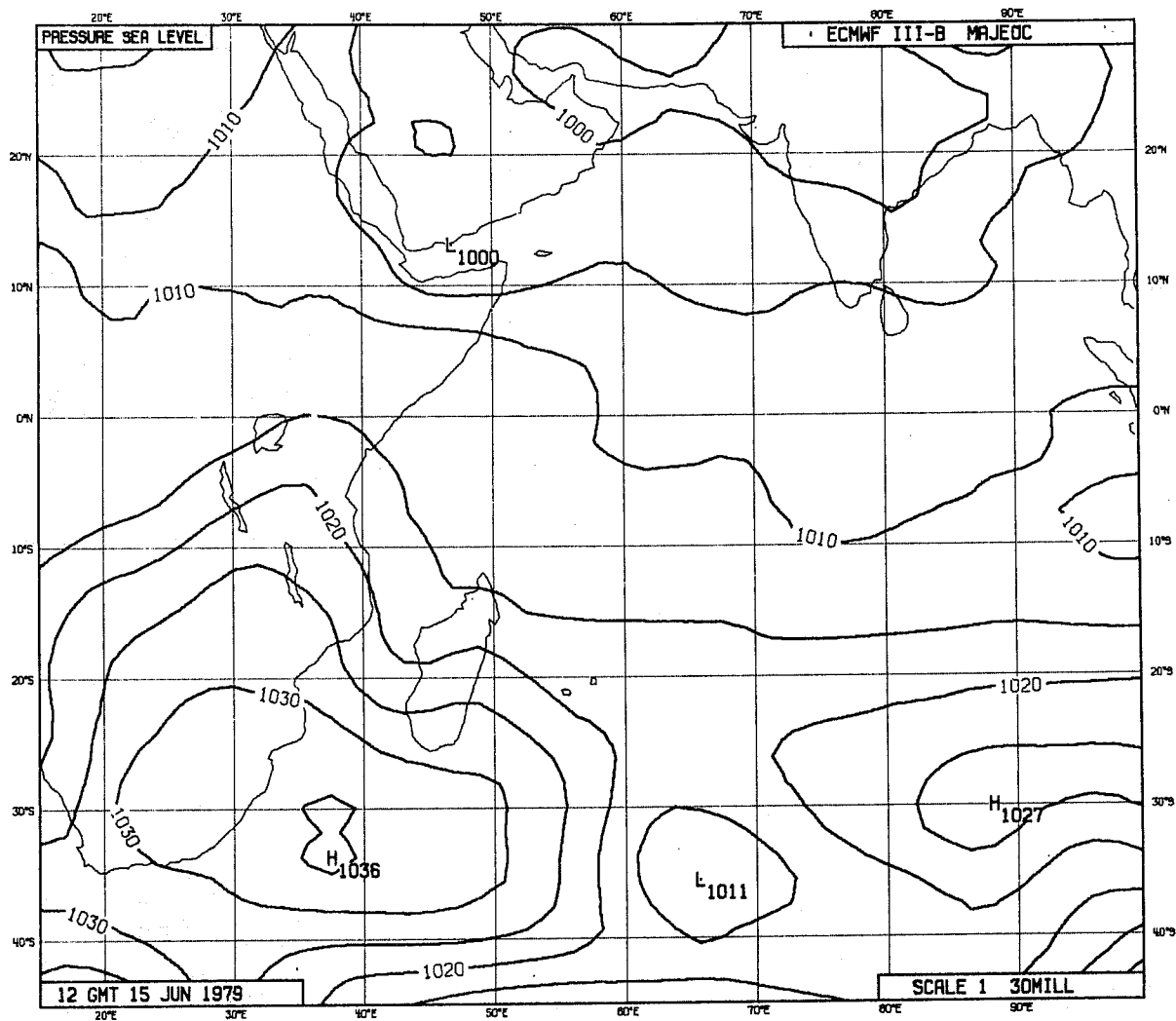


Fig. 3 As Fig. 1 but 12 GMT 15 June 1979.



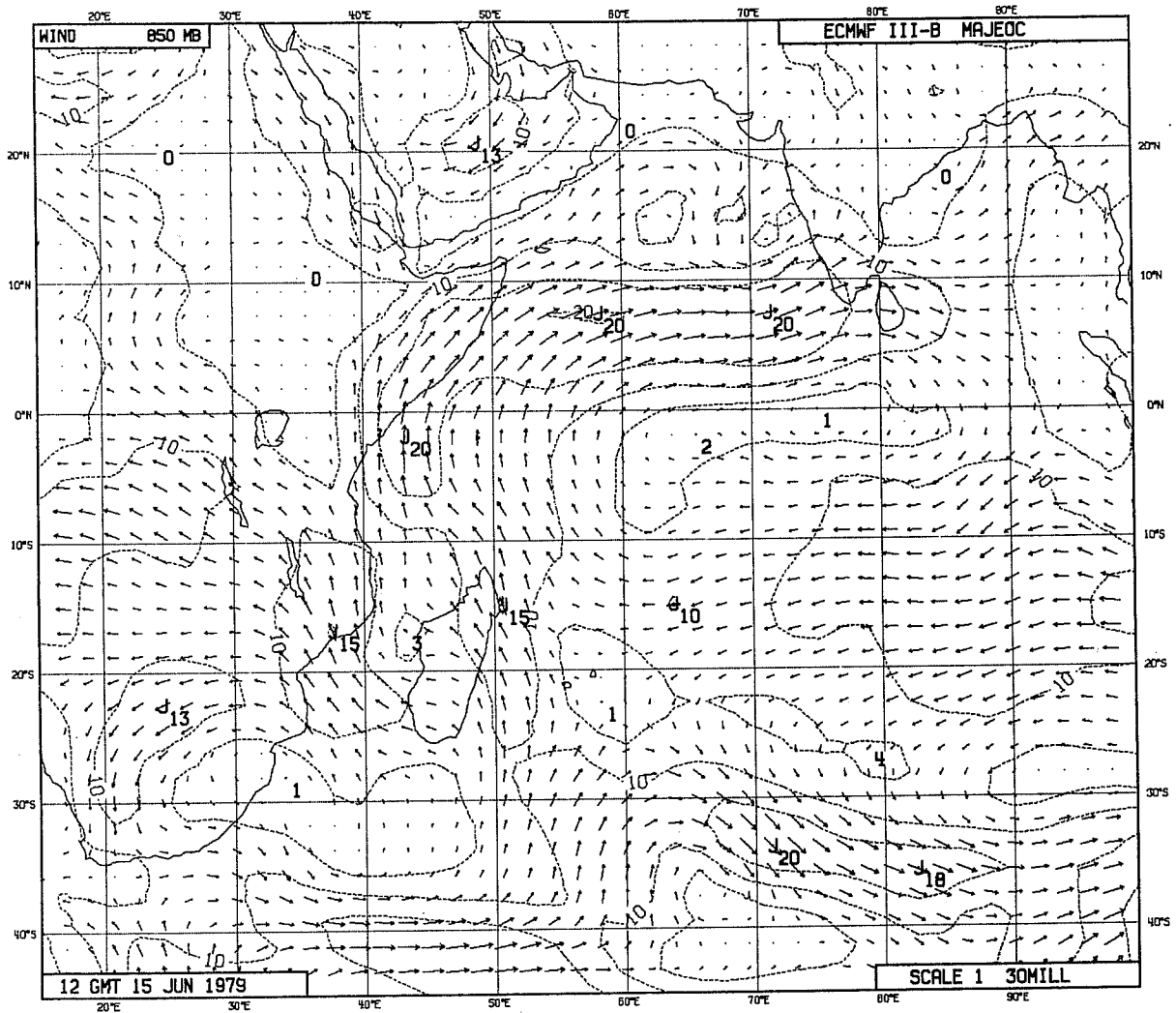


Fig. 4 As Fig. 2 but 12 GMT 15 June 1979.

11 JUNE 1979 12 GMT

POT. TEMP. (K) WINDS (M/S)

0.5PA/S  
20M/S

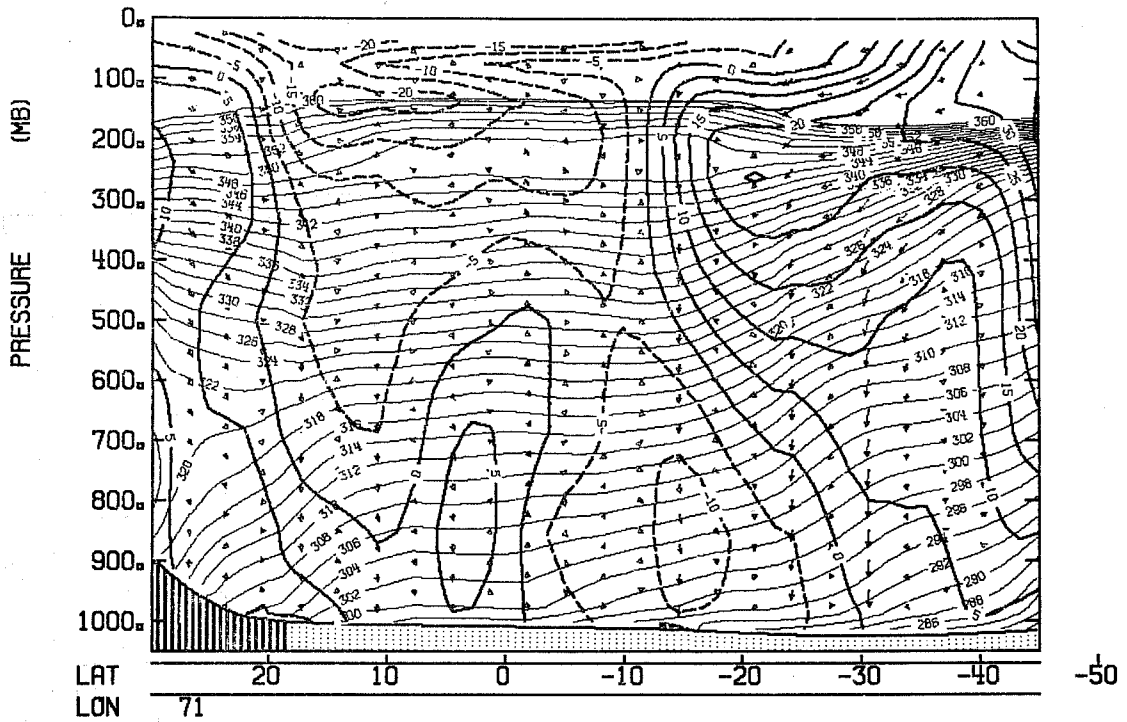


Fig. 5 Cross-section along 71°E for 12 GMT 11 June 1979. Thin lines potential temperature. Thick lines isovels (dashed for easterlies). The arrows indicate uninitialed vertical velocities.

15 JUNE 1979 12 GMT

POT. TEMP. (K) WINDS (M/S)

0.5PA/S  
20M/S

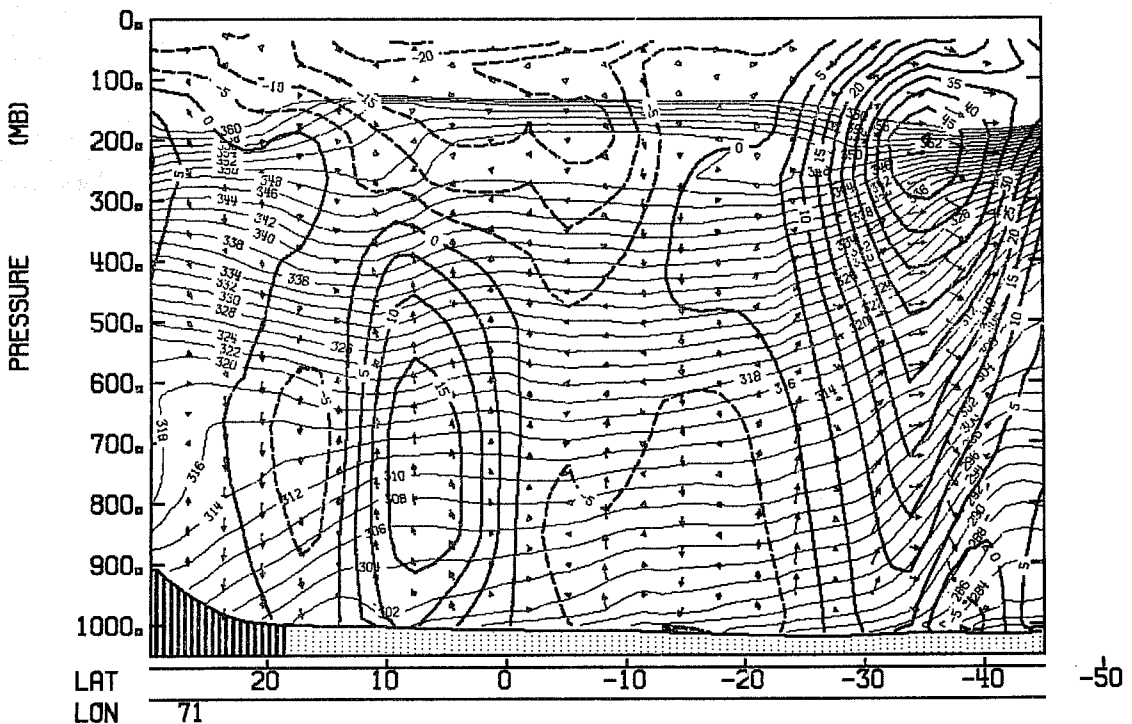


Fig. 6 As Fig. 5 but 12 GMT 15 June 1979.

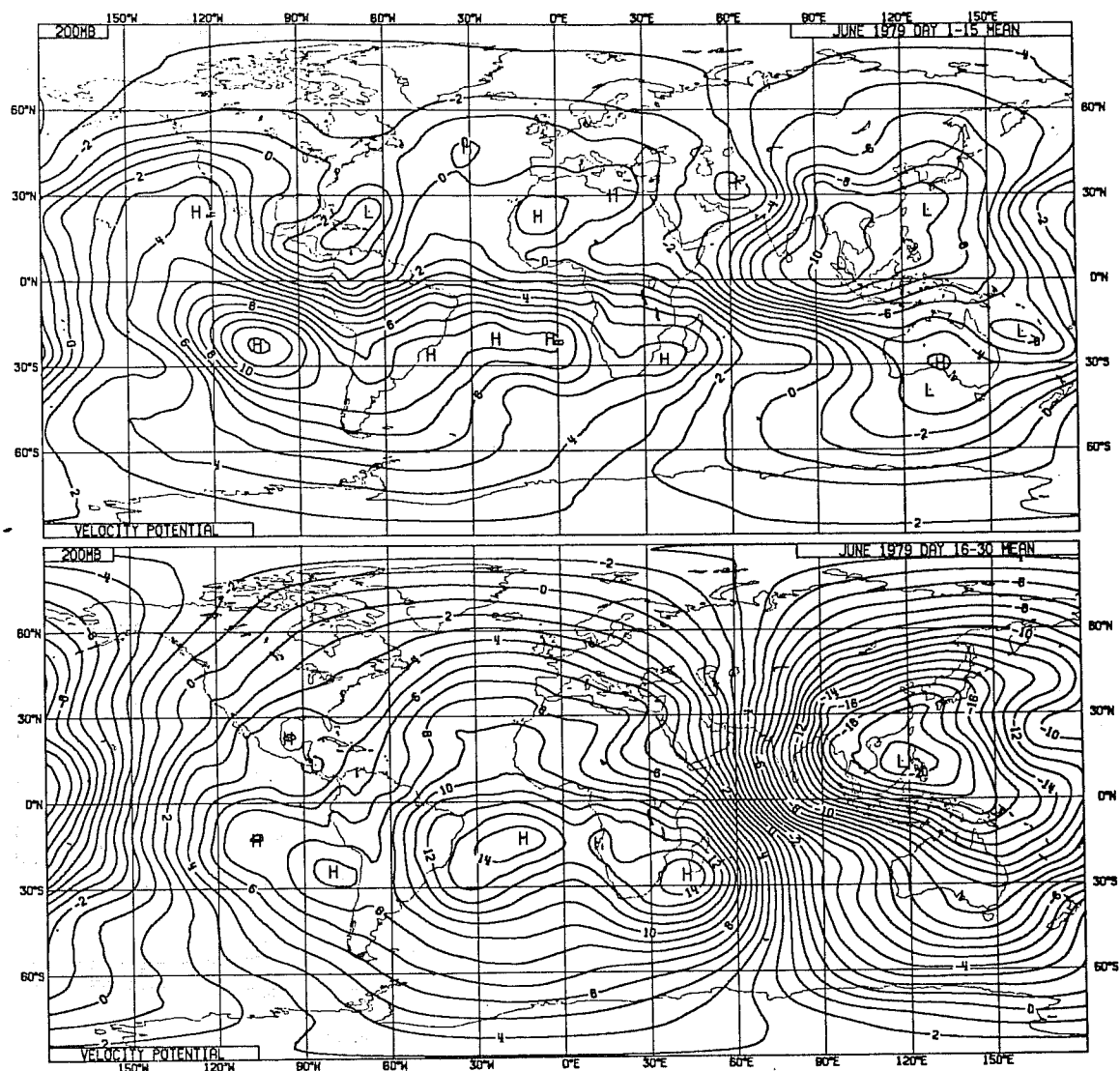


Fig. 7 Mean 200 mb velocity potential, 1-15 June (top) and 16-30 June (bottom).

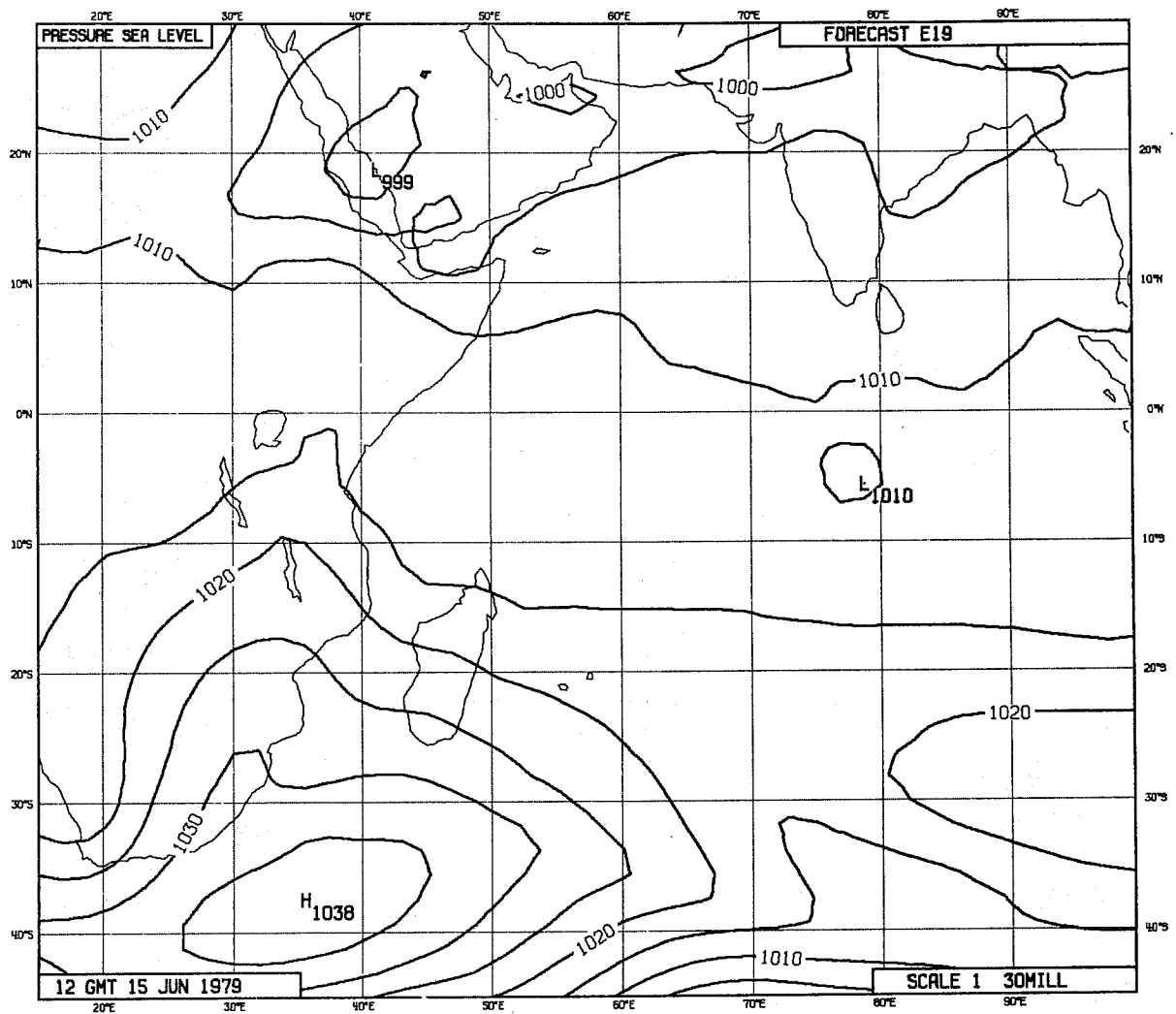


Fig. 8 Mean sea level pressure forecast, valid 12 GMT 15 June.  
 Initialized startfield.

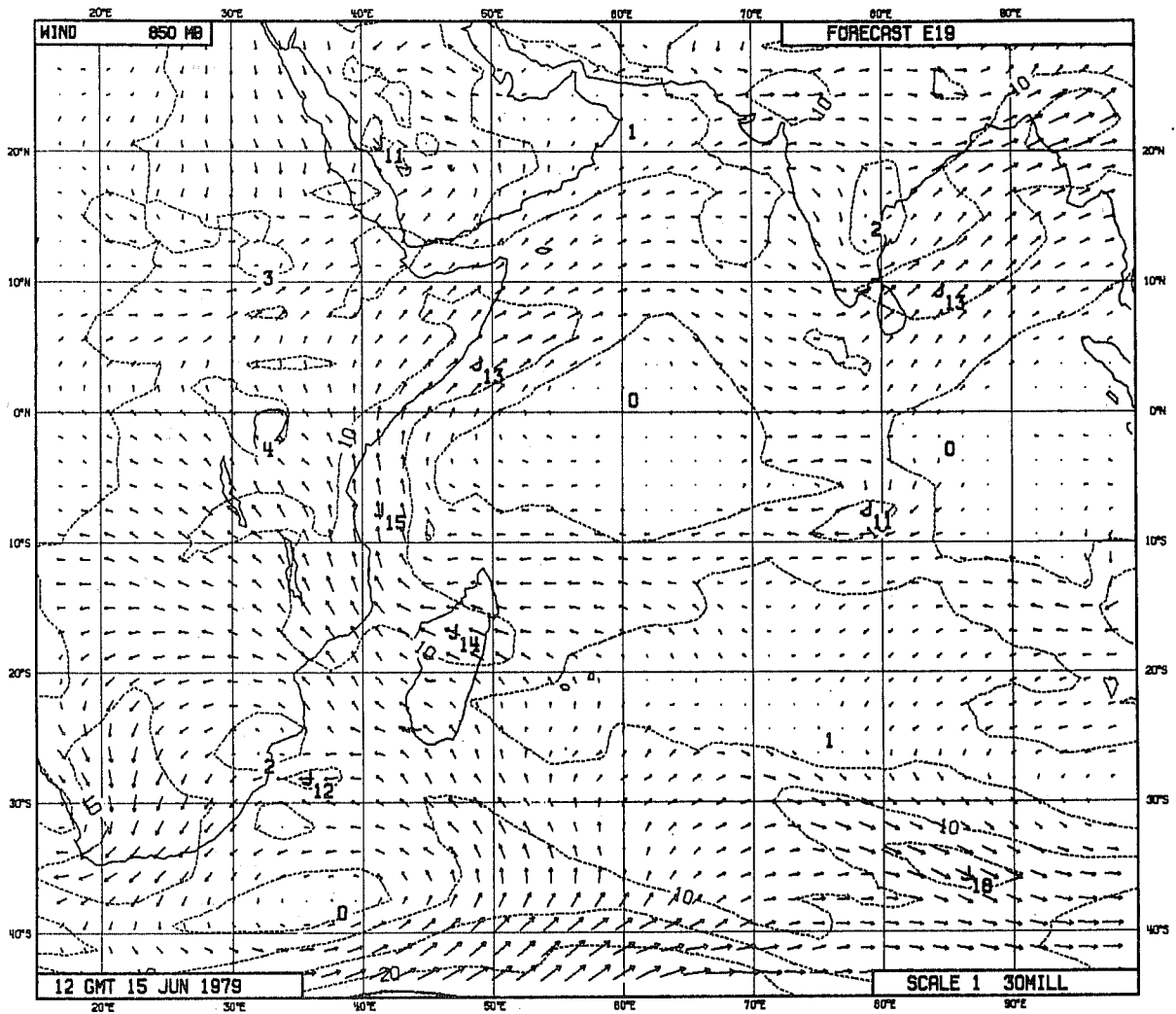


Fig. 9 850 mb wind forecast, valid 12 GMT 15 June 1979.

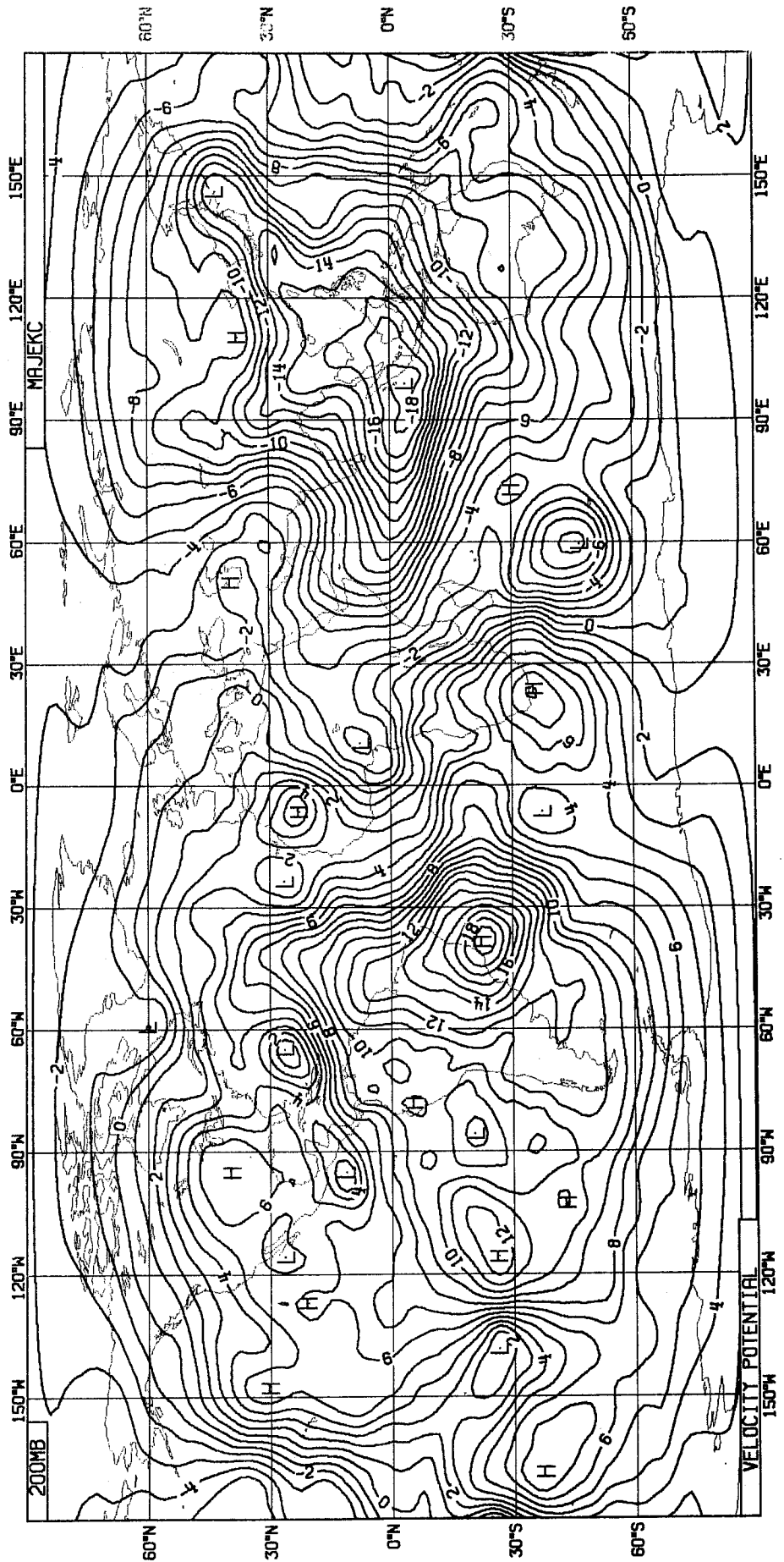


Fig. 10 200 mb velocity potential, 12 GMT 11 June 1979 before initialization.

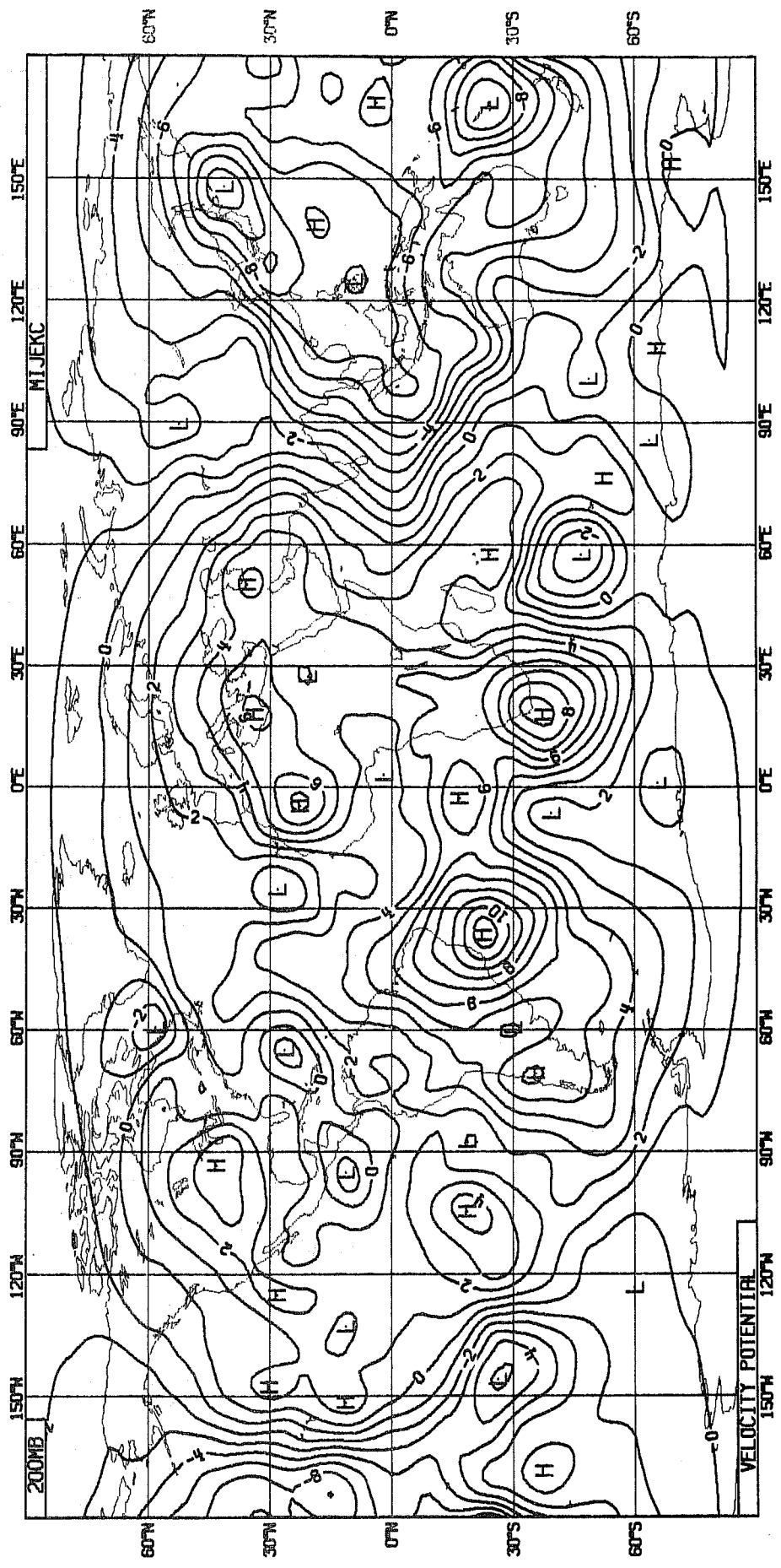


Fig. 11 As Fig. 10, but after initialization.

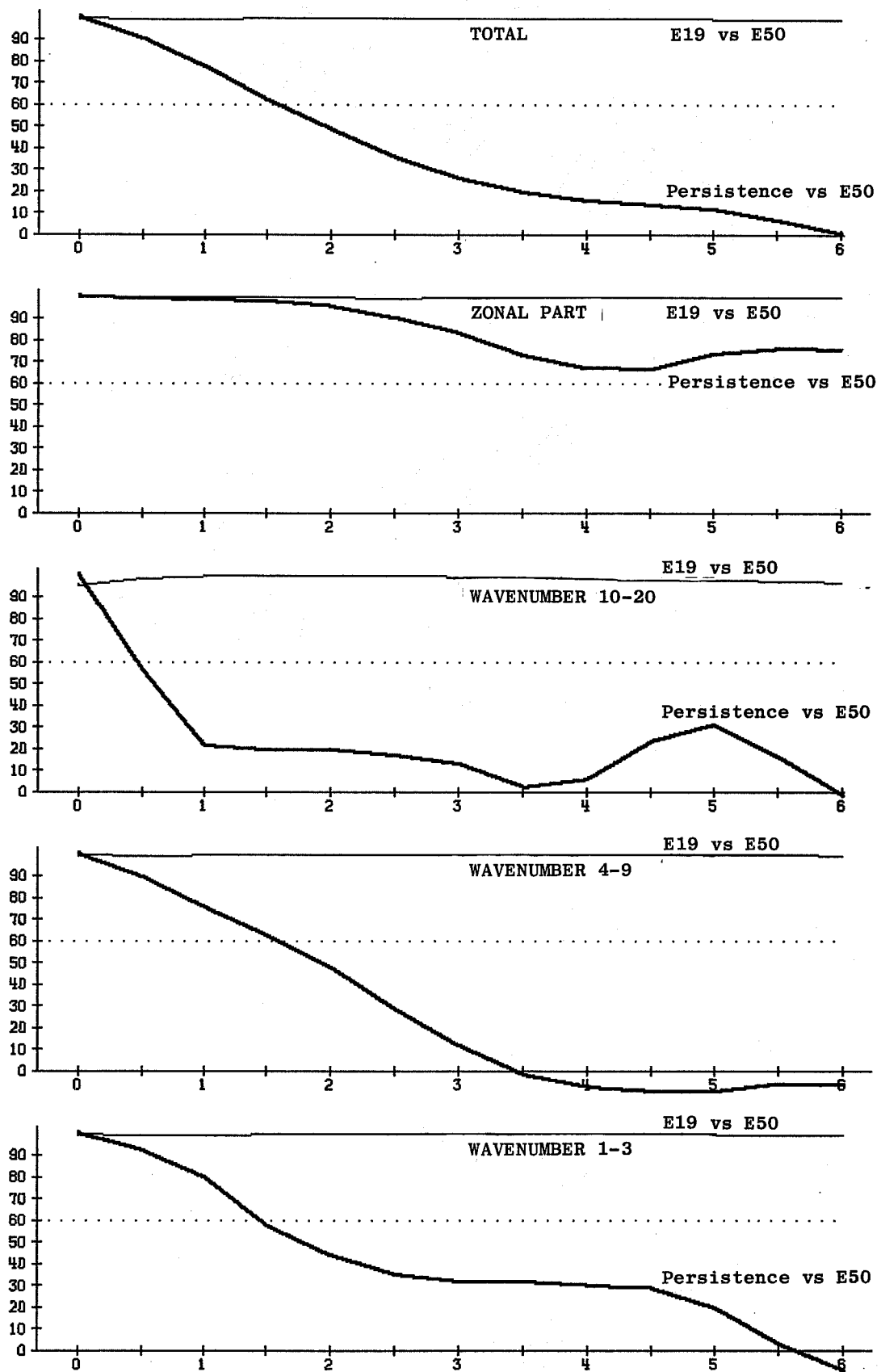


Fig.12 Relative anomaly correlation between the initialized (E19) and the uninitialized (E50) forecast.



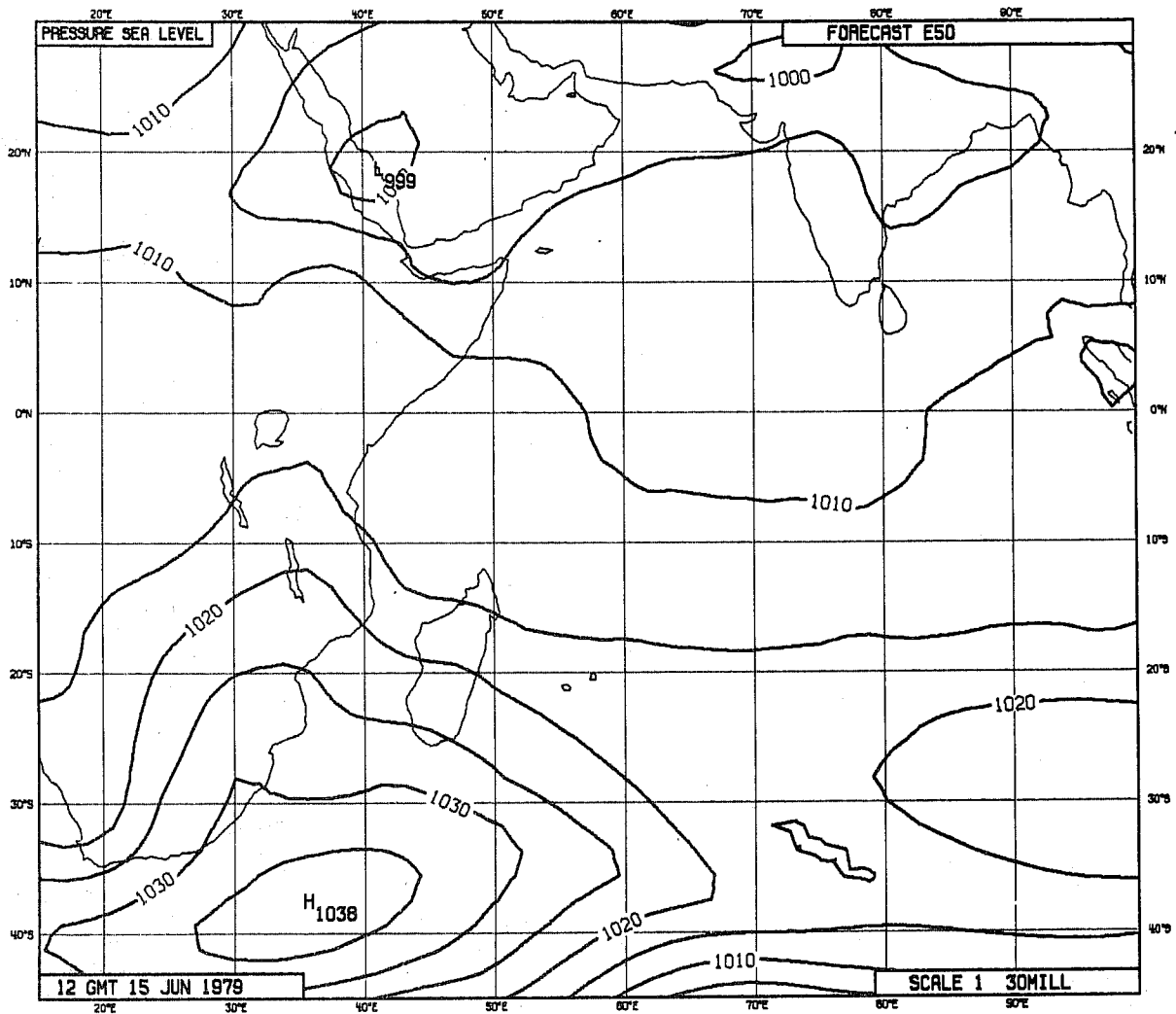


Fig. 13 As Fig. 8, but uninitialized startfield.

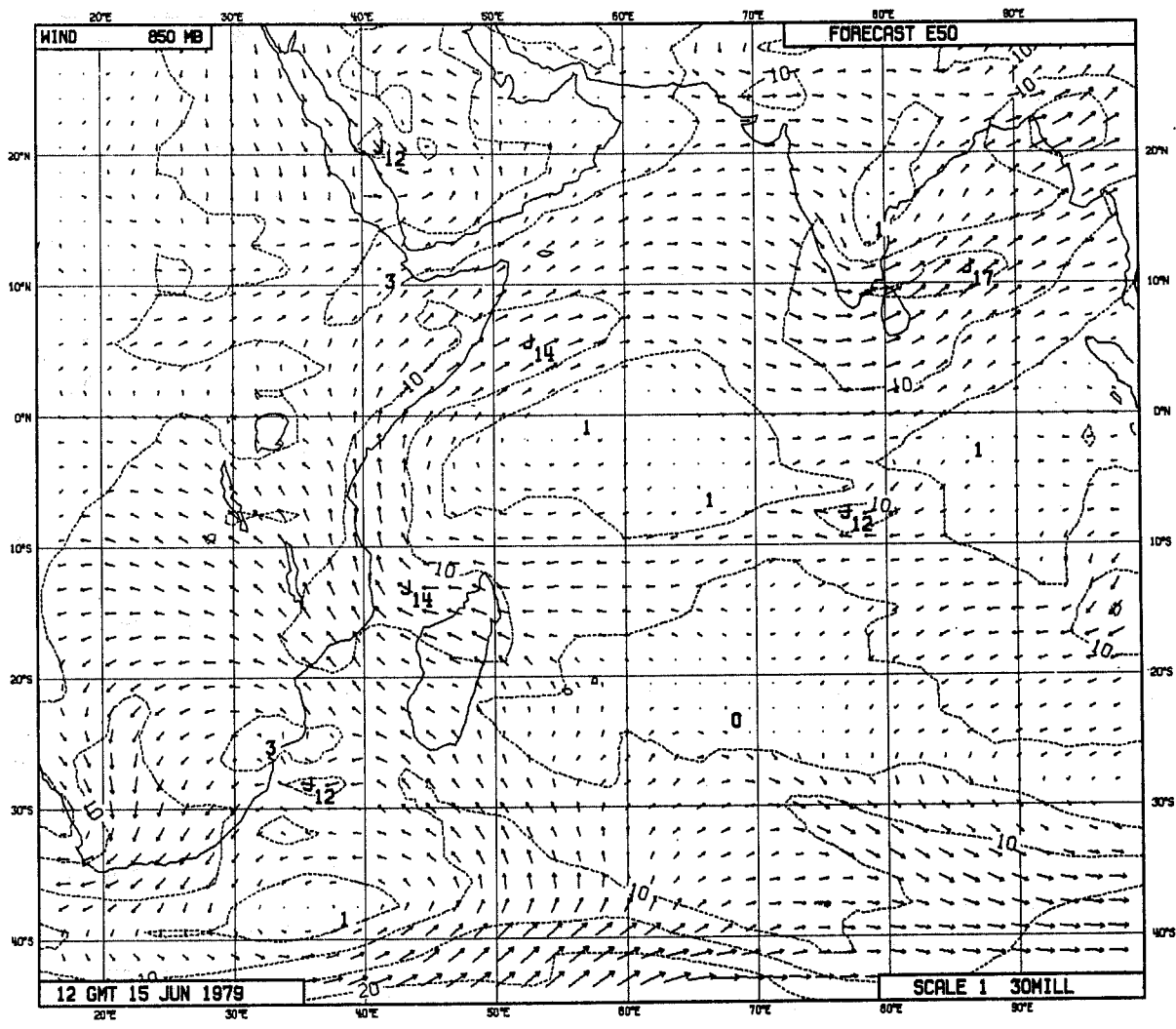


Fig. 14 As Fig. 9, but uninitialized startfield.

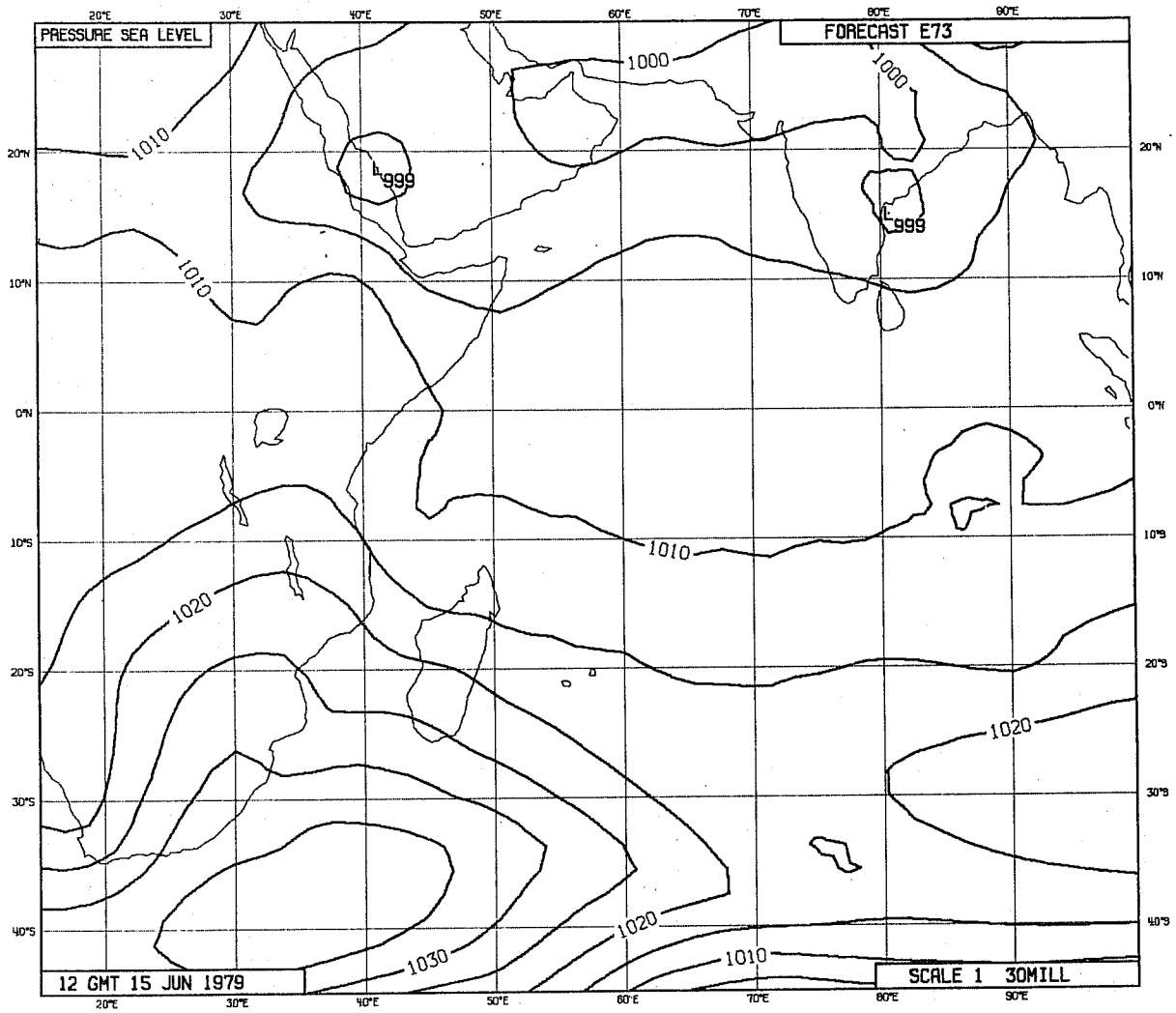


Fig. 15 As Fig. 8, but with "b" = 0

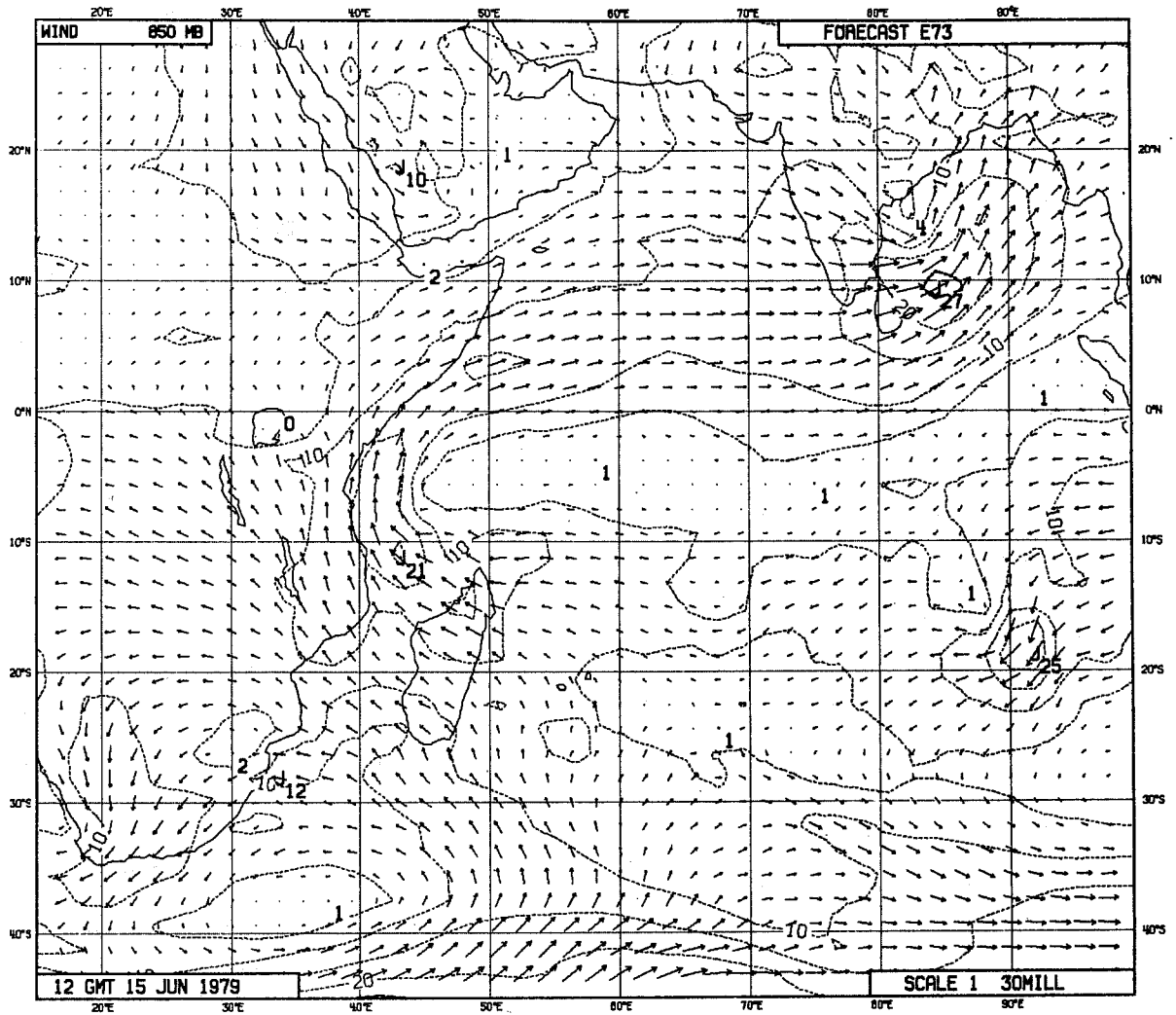


Fig. 16 As Fig. 9, but with "b" = 0